Electrophoresis of electrostatically assembled fullerene–porphyrin conjugates

Uwe Hartnagel, Domenico Balbinot, Norbert Jux* and Andreas Hirsch*

Received 26th January 2006, Accepted 13th March 2006
First published as an Advance Article on the web 31st March 2006
DOI: 10.1039/b601257d

The formation of electrostatically coupled assemblies of a series of anionic dendritic fullerene derivatives and cationic porphyrins in buffered aqueous media was studied with gel electrophoresis. Of central interest in these investigations was the variation of the amount of charge carried by the molecules, their size, shape and self-aggregation. Ferric cytochrome c **1** and the more rigid zinc porphyrin **2** served as octacationic species. The two new anionic fullerene derivates **3** and **6** were synthesized. The formation of electrostatic complexes of the fullerene polyelectrolytes **3** and **4** with **1** and **2** was clearly evident in the gel electrophoresis experiment. Compounds **5** and **6** showed a similar behaviour towards **2**. The electrophoresis experiments confirmed previous results obtained with other techniques on a qualitative level and gave new insights into aggregation phenomena.

Introduction

Coulomb interactions are of fundamental importance in nature and are employed in several facets in biological systems. They provide, for example, the electrostatic environment of proteins, which, in turn, governs their conformations, their binding affinities to other proteins and their reactivities towards substrate molecules. Mitochondrial cytochrome c **1** (Fig. 1), a polycationic redoxprotein which is present in many biological electron transfer processes, can be regarded as an excellent example demonstrating the above-mentioned principles. Consequentially, the hybridization of proteins with molecules that modify their function in terms of electron transfer[1] and conformational behaviour[2] is currently an important topic within bioorganic chemistry. Such aggregation phenomena and their concomitant electron transfer events are of elementary interest not only due to their obvious importance in nature but also as guiding principles in materials sciences.[3]

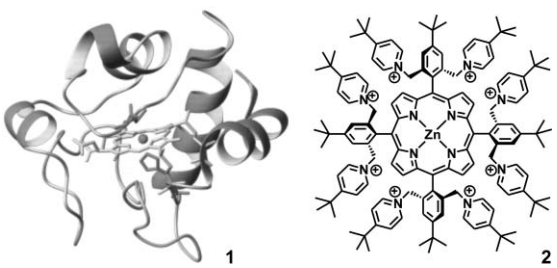

Fig. 1 Cytochrome c **1** and zinc porphyrin **2** (counterions not shown).

We discovered recently that a dendritic fullerene monoadduct in its eight-fold deprotonated state efficiently hybridizes with **1**, which carries eight positive charges in the outer periphery (K_a $\sim 10^5$ M^{-1}).[4] Furthermore, this fullerene derivative forms strong complexes with the octacationic zinc porphyrin **2** (K_a $\sim 10^8$ M^{-1}), which can be regarded as a biomimetic model system for **1**.[5] In recent studies, multicomponent electron transfer systems consisting of porphyrin polyelectrolytes, fullerenes and solubilized nanotubes were generated on the basis of electrostatic principles.[6] Very important analytical tools for all of these investigations are time-resolved fluorescence measurements and transient UV/Vis spectroscopy. The composition and association constants of electrostatically coupled hybrids were determined with these methods; unfortunately, they do not offer much help in analyzing the influence of size, shape and rigidity of the partners in the complex formation. Here, electrophoresis as the major analytical method for polyelectrolytes may help. This technique is commonly used in biology and biochemistry to evaluate the purity and the composition of charged biomolecules like DNA and proteins. For determining the purity of synthetic oligoelectrolytes, electrophoresis has been used much more rarely.[7–13] Interestingly, only a few examples are known in the literature where complexation studies with synthetic oligoelectrolytes were performed with electrophoresis.[7,13] Buchler *et al.* investigated the electrophoretic properties of polyanionic and polycationic porphyrins. In these studies, porphyrins were taken which carried typically only 4 positive or negative charges sitting in the porphyrin plane. These compounds had therefore just a two-dimensional topology.[8] Later on, this group investigated the complexation behavior of cationic cerium(III/IV) porphyrin double deckers with anionic metal porphyrinates and indigosulfonates.[9] Interestingly, one of the major results of these experiments was that electroneutrality is not a determining factor for the stoichiometry of aggregates. Mayburd *et al.* showed that bromophenol blue forms 1 : 1 complexes with ferric cytochrome c′ in gel electrophoresis, and attributed the complex formation to hydrophobic and not electrostatic effects.[13] Obviously, hydrophobic aggregation phenomena must be taken into account when studying electrostatically coupled polyelectrolytes.

We became interested in electrophoresis because we wanted to evaluate its usefulness as a tool in analyzing the aggregates of porphyrins and fullerenes in aqueous media. More specificially, what information can be extracted from the gel plates after electrophoresis and to what extent are the data in accord with results from the aforementioned photophysical studies?[4,5] It is

Institut für Organische Chemie, Universität Erlangen-Nürnberg, Henkestraße 42, 91054, Erlangen, Germany. E-mail: andreas.hirsch@chemie.uni-erlangen.de, norbert.jux@chemie.uni-erlangen.de; Fax: +49 9131 8526864; Tel: +49 9131 8522537

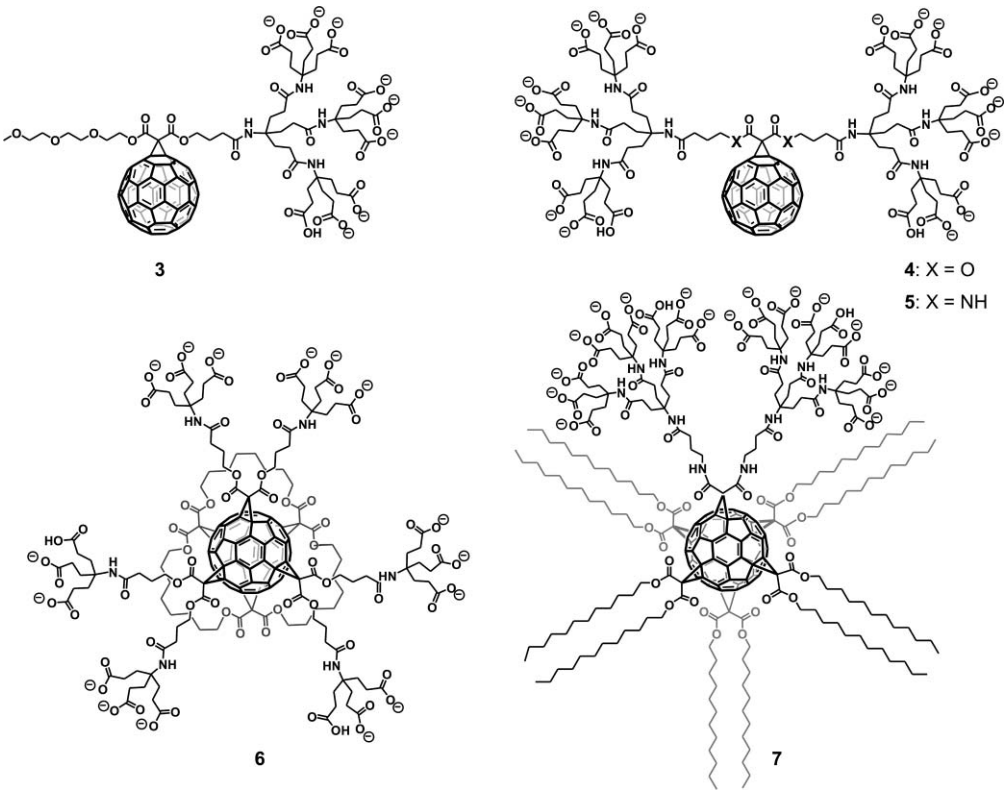

Fig. 2 Water-soluble anionic fullerene derivatives **3**, **4**,[14] **5**,[15,16] **6**, and **7**.[16]

of particular importance to us to see possible differences in the aggregation behaviour, when the compounds themselves tend to form micelles or other assemblies.

In this work we present electrophoresis experiments on the hybridization of cytochrome c **1** with the polyanionic dendritic fullerenes **3–7** (Fig. 2) as well as aggregation studies of an octacationic porphyrin **2** with these fullerenes. In order to investigate a broader range of compounds which vary in rigidity, amphiphilicity and the number of charges, we synthesized two new fullerene derivatives, **3** and **6**.

Results and discussion

1. Synthesis of new water-soluble dendrofullerenes 3 and 6

As just mentioned, the electrophoresis experiments on the formation of electrostatically coupled porphyrin–fullerene complexes required the synthesis of some new fullerene derivatives. Therefore, we decided to prepare the hitherto unknown fullerene oligoelectrolytes **3** and **6**, and thus complete a collection consisting of five fullerene derivatives (**3–7**, see Fig. 2).

The synthesis of the new water-soluble monoadduct **3** was performed according to Scheme 1. Mono-spacer malonate **10** can be synthesized in 50% yield through the esterification of malonic acid **8** with the spacer **9** using dicyclohexylcarbodiimide (DCC) as a coupling reagent. Compound **10** is a versatile building block for the synthesis of non-symmetrical malonates. Further esterification of **10** with triethylene glycol monomethyl ether yielded the unsymmetrical malonate unit **11**. Removal of the *tert*-butyl group followed by a modified Steglich coupling[17] of **12** with the well-known Newkome-type dendrimer H_2N–G2[18] gave the malonate-dendrimer **13**. After cyclopropanation, the neutral fullerene monoadduct **14** was obtained, which after acid-promoted removal of the *tert*-butyl groups led to the nona-acid **15**. At pH 7.2, **15** transforms into the octaanionic fullerene carboxylate **3** (Scheme 1). The triethylene glycol ether chain was thought to have a beneficial influence on the solubility of **3** in aqueous media. It turned out that **3** is more soluble in organic solvents compared to the corresponding monomethyl ester (not shown). In aqueous media **3** shows a higher tendency to form micelle-like species: DOSY (diffusion ordered spectroscopy) experiments proved that **3** forms small, weakly associated micelles at pH = 7.0 with a diameter of ~7–10 nm in 10^{-2} M solutions.

In order to guarantee an easy and regioselective access to the amphiphilic [3:3]-hexakis adduct **6** containing three pairs of dendritic units, we used the *eee*-trisadduct **18**, which was prepared according to a procedure that we developed previously.[19] The octahedral addition pattern was completed by DMA-templated cyclopropanation[20] using an excess of malonate **17** to yield the precursor fullerene **19** (Scheme 2). An important modification was the use of the phosphazene P_1-base for the cyclopropanation, because with the typically applied 1,8-diazabicyclo-[5.4.0]undec-7-ene (DBU) only nonsymmetrical tetraadducts were obtained. P_1, also called the Schwesinger base,[21] is a neutral nitrogen base which is approximately 2000 times more basic than than DBU and also more sterically hindered. For a Bingel cyclopropanation, the P_1-base was diluted in CH_2Cl_2 and added dropwise to the reaction mixture. The usage of sterically demanding malonates for the synthesis of mixed [3:3]-hexakis adducts often leads to an

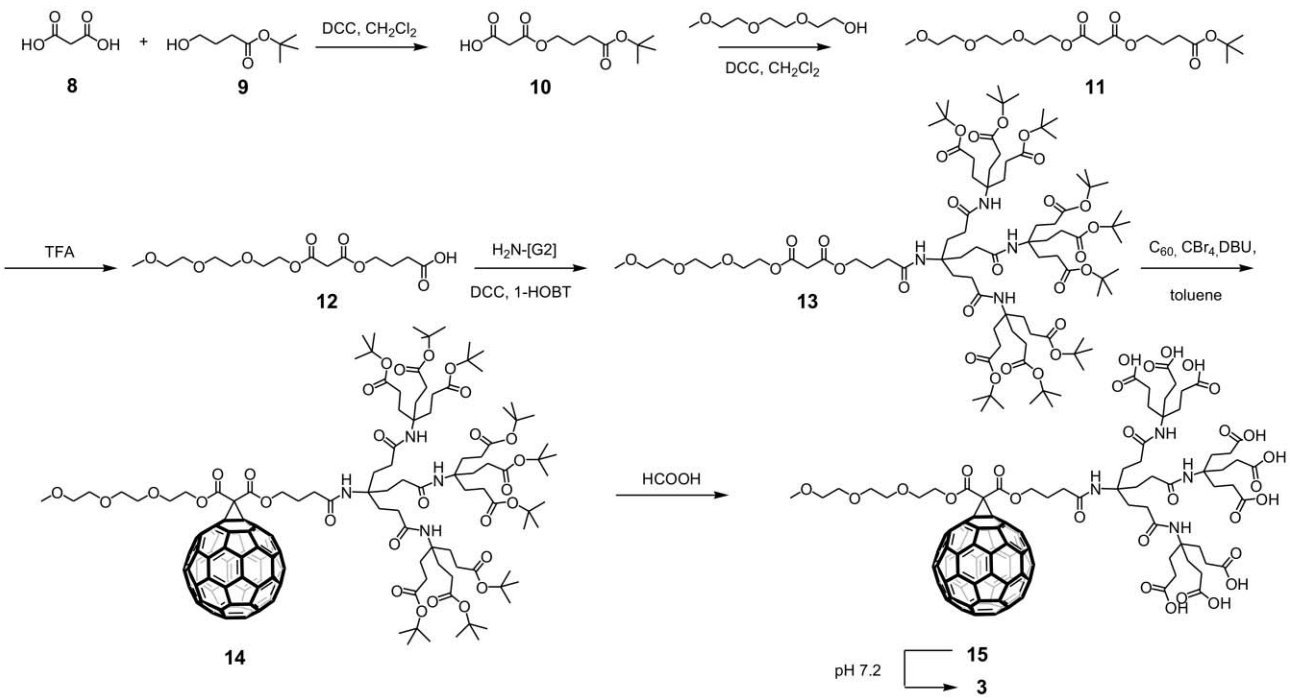

Scheme 1 Synthesis of the new water-soluble dendrofullerene **3**; H_2N–G2 = second generation Newkome dendrimer.

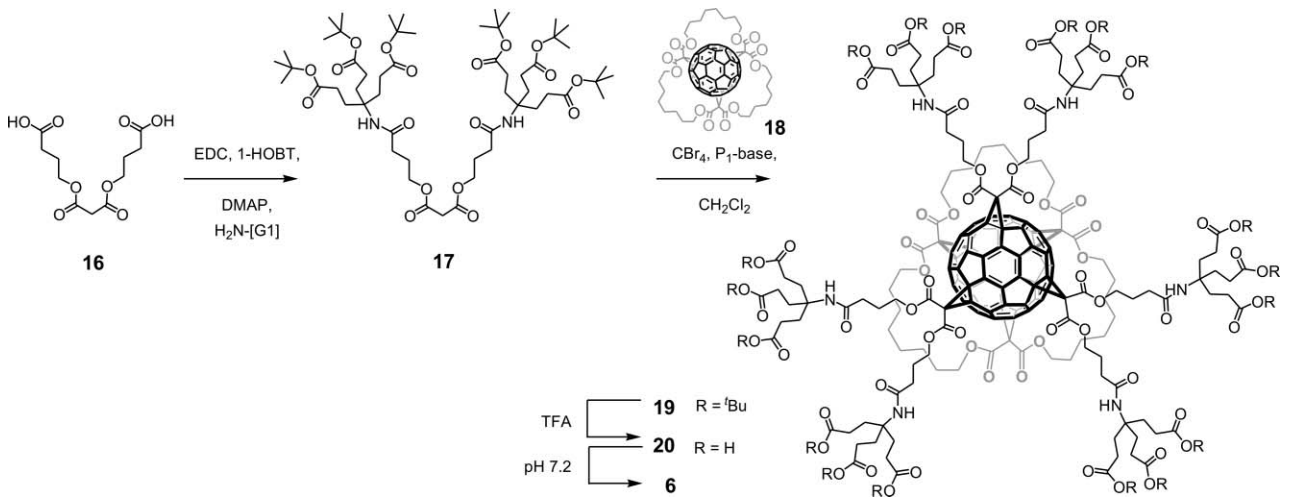

Scheme 2 Synthesis of the new water-soluble [3:3]-dendrofullerene **6**; P_1-base= *N‴*-*tert*-butyl-*N*,*N*,*N′*,*N′*,*N″*,*N″*-hexamethylphosphorimide triamide.

incompletely octahedral addition pattern. HPLC analysis showed the appearance of tetrakis and pentakis adducts with a non-equatorial addition pattern. In such cases, using the phosphazene base tends to result in much better yields of the desired hexakis adducts.[22] Removal of the *tert*-butyl groups of **19** was achieved with TFA, leading to the octadeca-acid **20**. Titration experiments have shown that upon dissolving **20** in a buffered solution of pH 7.2, the hexadecaanion **6** is predominant, beside other less deprotonated species. This salt is not isolated and exists as such only in solution. DOSY measurements clearly show that **6** forms aggregates with a diameter of ~8–10 nm in concentrated solution ($\sim 10^{-2}$ M). At lower concentrations smaller complexes are formed, presumably an equilibrium mixture between aggregates containing two or four units of **6**.

2. Complexation studies

In complexation studies, cytochrome c **1** acts as a large and flexible partner in electrostatic assemblies, with a mass of approximately 13 kDa and carrying eight positive charges.[2] The octacationic zinc porphyrin **2** serves as an example for a more rigid and rather small, highly charged porphyrin system that can adopt a double-cone conformation. Although both compounds **1** and **2** are similarly charged, hybrids of **1** will be dominated in shape and structure by the size of **1**, whereas the much smaller **2** with its higher local concentration of the positive charges will give rise to much more dense assemblies.

A collection of anionic fullerene electrolytes, namely the amphiphilic fullerene carboxylates **3–7** (Fig. 2), were chosen as

oppositely charged species for the complexation studies with **1** and **2** (Fig. 1). The fullerene monoadduct **3** has a dendritic part which carries nine carboxylic acid groups. Titrations performed in order to analyze the range of pK_a values of the carboxylic acid groups revealed that **3** possesses eight negative charges at physiological pH in water. In other words, the major species present in the mixture is the octaanionic form of **3**.[23] This seems to be a typical trait of this Newkome-type dendrimer branch. Compounds **4** and **5** have two of these dendritic arms, and therefore carry 16 negative charges at pH 7 – determined again by pH titrations. The difference between **4** and **5** is the connection of the dendritic parts to the fullerene moiety. For **4**, the connecting group is an ester group that has more rotational freedom than the amide group in **5**, which certainly influences the overall rigidity of both molecules. DOSY measurements show that **3**, **4** and **5** form small, weakly associated micelles at pH = 7.0 with a diameter of ~7–10 nm in 10^{-2} M solutions. We expected that in complexation experiments of **3–5** with **1** or **2**, these micelles could break apart to give the monomeric species, which would then undergo aggregate formation. Because monomer and oligomer(s) are in equilibrium, this would also lead to a leaching of the oligomeric species. The hexakis adducts **6** and **7** have also sixteen negative charges at physiological pH, albeit with a considerably different spatial distribution than **3–5**. The additional modification of the fullerene core with non-polar groups leads to an enhanced amphiphilic character. In particular, **7** possesses an average dimension of about 3.5 nm along the main polar axis,[16] which is similar to that of natural phospho- or glycolipids. Further details on the aggregation behaviour of **7** were revealed by ultrafast cryogenic fixation and direct observation by transmission electron microscopy. At pH 7.2 (phosphate buffer) **7** dissolves and forms predominantly rod-shaped aggregates with a double-layer ultrastructure. The diameter of these rods is 65 ± 5 Å whereas their lengths vary considerably. At pH 9.2 (borate buffer) only globular micelles with a diameter of 85 ± 10 Å are formed.[16] By using reconstruction techniques the three-dimensional structure of these globular species was determined to consist of eight units of **7**. It should be pointed out that the concentration of **7** used in this study was about a factor of 100 higher than that used for the electrophoresis experiments.

The various species in the gel electrophoresis experiments were detected by three different optical filters [short-pass (sp) 500–550 nm, medium-pass (mp) 550–610 nm and long-pass (lp) 600–650 nm filters] which allowed for the selective visualization of fullerenes *vs.* porphyrins. This is particularly useful in those cases in which the very strong fluorescence of porphyrin **2** is dominant on the gel plates.

So far, we have not succeeded in reproducing the electrostatic complexation of charged fullerenes with porphyrins with mass spectrometric methods such as ESI or MALDI-TOF.

2.1 Aggregation of the octacationic cytochrome c 1 with anionic dendrofullerene 3. Pure cytochrome c **1** shows only one sharp spot in the cathodic region, but with a significantly smaller migration speed (Fig. 3) than cationic porphyrin **2** (see Section 2.3) – an unsurprising result because of the much larger size of **1**. Detection of pure **1** is only possible with the medium-pass filter, with which it can be detected up to a dilution factor of 1 : 10 (1×10^{-4} M).

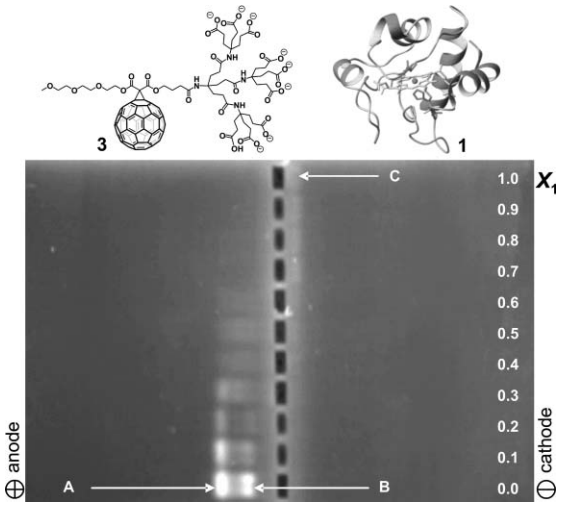

Fig. 3 Flat gel electrophoresis (PA-gel plate 100 mm × 65 mm × 5 mm; phosphate buffer, pH 7.2, 300 V, 12 mA, 273 K, 20 min) of a mixture of water-soluble dendrofullerene **3** and cytochrome c **1** with increasing molar fraction of protein X_1. Detection was performed with a long-pass filter. Gel pockets in the middle mark the starting points of electrophoresis. **A** and **B**: **3** migrates to the anode; **C**: **1** migrates to the cathode.

Due to the iron center, the heme's fluorescence is quenched and detection of cytochrome c **1** with UV light is very difficult over the whole scale of the molar fraction X_1. Indeed, only a barely visible band **C** can be found at high X_1 values. Therefore, only the fluorescence of fullerene **3** was used to detect aggregation phenomena. A dilution series performed with pure **3** showed that its detection with UV light is possible up to a concentration of 6.6×10^{-5} M. Interestingly, pure **3** splits into two bands (**A** and **B**) on the gel. Because **3** was freshly prepared and analytically pure, the existence of two bands indicates the presence of an aggregate (band **B**) which is in equilibrium with monomeric **3** (band **A**). Similar dendrofullerenes are known to form oligomers at lower pH values through their fullerene surfaces,[23] although at much higher concentrations. It seems possible that under the given conditions a tetrameric species may be formed.

With increasing amounts of **1** the slower band **B** disappears, whereas **A** seems to be somewhat more persistent but vanishes also at $X_1 = 0.3$–0.4. Only monomeric **3** forms complexes with **1**, removing them from the equilibrium, and thus **A** slowly diminishes also. At $X_1 = 0.4$–0.5 the fullerene species have completely disappeared, which makes the formation of a 1 : 1 complex between **1** and **3** plausible. Quite obviously, the fullerene fluorescence is quenched with rising X_1. The apparent lack of strong fluorescence makes a clear assignment of complex formation between **3** and **1** difficult. Nevertheless, this experiment clearly reproduced the formation of complexes of cytochrome c with anionic fullerenes that we reported earlier.[4] Further, the diffuse transition between $X_1 = 0.4$–0.6 can be understood in that the complex between **1** and **3** is less stable than the one with the smaller and more rigid octacationic porphyrin **2**.[4,5]

2.2 Aggregation of cytochrome c 1 with hexadecaanionic dendrofullerene ester 4. Our next step was the investigation of the complexation behaviour of the water-soluble dendrofullerene **4**, which carries two dendritic branches. Due to the repulsive charges on its arms, the two branches tend to spread away from each other.

Complexes of **4** with **1** may possess 1 : 1 or 1 : 2 ratios which should have different migration speeds in gels due to their different size and total charge. Compound **4** also shows two sharp bands (**A** and **B**) in the anodic region (see Fig. 4). The migration distance of **4** is much larger than **3** because of the higher charge. Band **A** shows a higher fluorescence intensity than band **B**, independent of the filters used. Both **A** and **B** of pure **4** are detectable up to a dilution of 1 : 20 (5×10^{-5} M) with all filters, and not only with the short and medium-pass filters, as was the case with **3**. Obviously, different types of addends can change the fluorescence properties because they influence self-aggregation. The two detected bands of the pure fullerene compound **4** clearly show the equilibrium between single entities (**A**) and discrete oligomeric species (**B**). The existence of such aggregates at higher concentrations than used here can be demonstrated by DOSY through measurements in D_2O at pH 7.2.

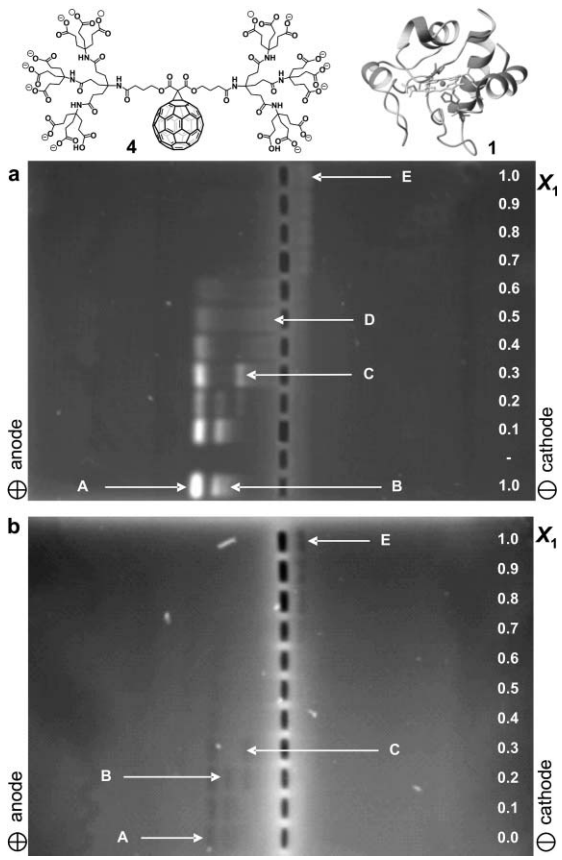

Fig. 4 Flat gel electrophoresis (PA-gel plate 100 mm × 65 mm × 5 mm; phosphate buffer, pH 7.2, 300 V, 12 mA, 273 K, 20 min) of a mixture of water-soluble dendrofullerene **4** and cytochrome c **1** with increasing molar fraction of protein X_1. a) Short-pass filter. b) Long-pass filter. Gel pockets in the middle mark the starting points of electrophoresis. **A** and **B**: **4** migrates to the anode; **C** and **D**: anionic Coulomb complexes migrate to the anode; **E**: **1** migrates to the cathode.

Fig. 4 shows the complexation studies with **4** and **1** observed through a short-pass filter (Fig. 4a) and a long-pass filter (Fig. 4b). The latter allows the selective detection of the porphyrin's fluorescence, whereas the short-pass filter cuts this fluorescence off. As was found for the fullerene carboxylate **3**, the C_{60} hexadecakis carboxylate **4** shows two distinct bands, **A** and **B**. The faster moving species **A** is detectable up to $X_1 = 0.6$. Spot **B** is only detectable up to $X_1 = 0.2$. A new band (**C**) with a smaller migration speed arises in the anodic region at a molar fraction X_1 of 0.2. It becomes more intense, with a maximum at $X_1 = 0.3$, and disappears completely at higher molar fractions. Band **C** may be an electrostatic 1 : 1 complex between **1** and **4**, because such a complex would possess an excess of negative charge, and therefore would migrate to the anode. Furthermore, the electrostatic coupling with **1** decreases the total charge of **4**, and consequently the complex should move slower than the free hexadecaanion **4** – which is indeed observed. A diffuse zone **D** from $X_1 = 0.3$ to $X_1 = 0.7$ can be observed, which may consist of higher aggregates with an excess of negative charge. In the cathodic region, spot **E** shows **1** up to a molar fraction X_1 of 0.5. The most striking observation in this experiment is the change at $X_1 = 0.7$, from which point onwards no fullerene can be detected on the anodic site. Here, we clearly see the formation of a 2 : 1 complex between **1** and **4**. A similar picture is found with the detection by the short-pass filter. This experiment demonstrates the existence of stable cytochrome c–fullerene aggregates under electrophoretic conditions.

2.3 Aggregation of the octacationic zinc porphyrin 2 with octaanionic dendrofullerene 3. Previous experiments have shown that complexes of a dendrofullerene similar to **3** with cytochrome c **1** or porphyrin **2**[4,5] are stable in water due to electrostatic interactions. Molecular dynamics calculations suggested that fullerenes such as **3** are not able to cover **2** completely but leave half of the molecule exposed.[5] Therefore, complexation of further polyelectrolytes such as another molecule of **3** should be possible. Formation of the 1 : 1 complex and possibly higher aggregates can indeed be visualized with PAGE (polyamide gel electrophoresis). It should be pointed out that the fluorescence intensities of the compounds on the plates change dramatically after prolonged exposure to UV light. Consequently, the apparent difference of the fluorescence of **3** on the gel plates shown in Fig. 3 and Fig. 5a is the result of different illumination times.

Figs. 5a and b show the same electrophoresis plate with long- and short-pass detection modes. As was described above (see Fig. 3), **3** shows two sharp bands, **A** and **B**, in the anodic region ($X_2 = 0$), with **B** being only detectable with the long-pass filter (see Fig. 5b). With increasing molar fraction of porphyrin **2**, band **A** fades out and band **B** becomes more intense; further migration of spot **B** becomes slower. Apparently, even small amounts of **2** have a much stronger influence on **3** than **1**. The appearance of the porphyrin's fluorescence on the anodic side even at low X_2 is a clear sign that **2** is transported to the anode as a Coulomb complex with an overall negative charge. This clearly proves the electrostatic complexation between **3** and **2**. At a molar fraction of $X_2 = 0.5$ bands **A** and **B** completely disappear and a new band **C** arises, which shows the most intense fluorescence in the anodic region and additionally has the shortest migration. Beginning with $X_2 = 0.6$, the porphyrin appears as band **D** in the cathodic region. Obviously, two different species are present in the region from $X_2 = 0.5$ to $X_2 = 0.8$, one of which is free porphyrin **2**. The other must be a negatively charged Coulomb complex of **2** and **3** which, by virtue of its total charge, cannot be the expected 1 : 1 complex. It is likely that **2** forms complexes with pre-formed aggregates of **3**. A closer look reveals small fluorescence spots in the gel pockets at $X_2 = 0.5$–0.8, which may indicate the precipitation of the expected

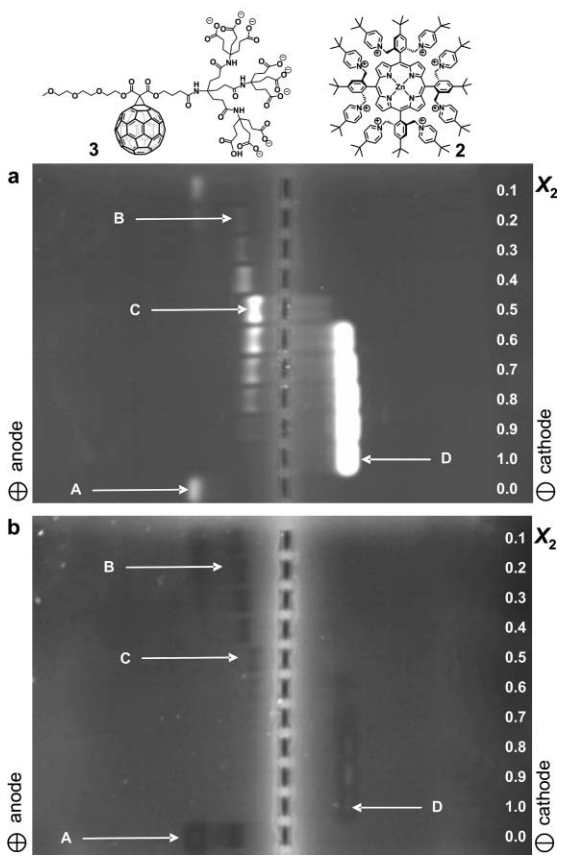

Fig. 5 Flat gel electrophoresis (PA-gel plate 100 mm × 65 mm × 5 mm; phosphate buffer, pH 7.2, 300 V, 12 mA, 273 K, 20 min) of a mixture of water-soluble dendrofullerene **3** and cationic zinc porphyrin **2** with increasing molar fraction of porphyrin X_2. a) Long-pass filter; b) Short-pass filter. Gel pockets in the middle mark the starting points of electrophoresis. **A** and **B**: **3** is migrating towards the anodic region; **C**: anionic Coulomb aggregates migrate to the anode; **D**: **2** migrates to the cathode.

1 : 1 complex between **2** and **3**. We do not believe that π–π-stacking interactions between the fullerenes and porphyrin **2** are possible. The pyridinium substituents of **2** prevent the close approach of the porphyrin ring system and the fullerene spheres because of the *ortho*-substitution pattern in **2**.

2.4 Aggregation of the octacationic zinc porphyrin 2 with hexadecaanionic dendrofullerene ester 4. The interactions of the cationic porphyrin **2** with the hexadecaanionic dendrofullerene **4** are shown in Fig. 6. Compound **4** shows a similar behaviour towards **2**, as was observed for **1** (see Fig. 4). Due to the strong fluorescence of **2**, the complexation events are easier to analyse. With increasing molar fraction X_2 of porphyrin **2**, the intensity of band **A** decreases until $X_2 = 0.4$, where its detection was no longer possible. Interestingly, a significant change appears at $X_2 = 0.4$, where **B** seems to be exchanged by a slower migrating species **C** that possesses a diffuse trail. It is possible that a 1 : 1 complex between **2** and **4** is formed at $X_2 = 0.4/0.5$ which carries an overall eight-fold negative charge and therefore moves towards the anode. As X_2 increases further, **C** becomes more and more diffuse until X_2 reaches 0.7, at which point it completely disappears. Paralleling the behaviour of **C** is band **D**, which may be a species similar to

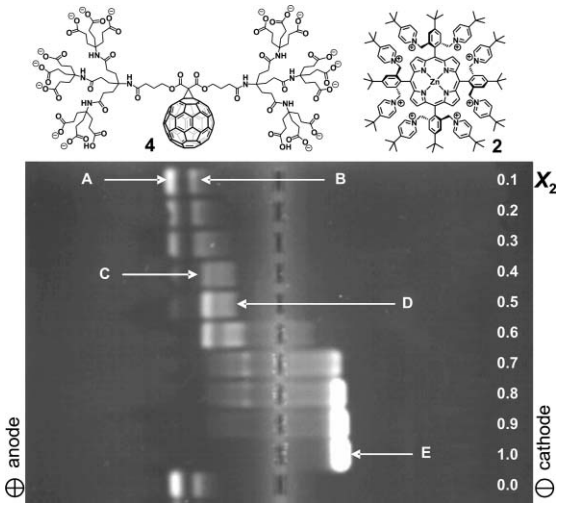

Fig. 6 Flat gel electrophoresis (PA-gel plate 100 mm × 65 mm × 5 mm; phosphate buffer, pH 7.2, 300 V, 12 mA, 273 K, 20 min) of a mixture of water-soluble dendrofullerene **4** and cationic zinc porphyrin **2** with increasing molar fraction of porphyrin X_2. Detection was performed with a long-pass filter. Gel pockets in the middle mark the starting points of electrophoresis. **A** and **B**: **4** is migrating towards the anodic region; **C** and **D**: anionic Coulomb aggregates migrate to the anode; **E**: **2** is migrating to the cathode.

that observed for **3**, that is, **2** forms complexes with pre-formed self-aggregates of **4**. The disappearance of both bands could be an indication for a breaking-apart of such assemblies. At $X_2 = 0.7$, a new band **E**, assumed to be non-complexed porphyrin **2**, appears in the cathodic region. Also, starting with $X_2 = 0.6$, the starting pockets show strong fluorescences, which are most likely due to a precipitation of the neutral 2 : 1 complex between **2** and **4**. This experiment clearly shows two distinct events on the electrophoresis plate, which can be attributed to the formation of a 1 : 1 and a 2 : 1 complex between **2** and **4**, respectively.

2.5 Aggregation of the octacationic zinc porphyrin 2 with hexadecaanionic dendrofullerene amide 5. The behaviour of **5** in association studies is more or less comparable to that of **4** (Fig. 7). Although **5** was expected to have fewer degrees of freedom due to the central amide bonds, its migration properties are similar to that of **4**. With increasing X_2 the situation becomes more complicated. In particular, band **C** consists now of two distinguished parts, whereas for the ester **4** it seemed to possess just a tail. The splitting of band **C** may indicate the presence of not only the well-defined 1 : 1 complex but also 2 : 2 or 2 : 3 complexes between **5** and **2**. Another remarkable difference is that here, band **D** is less diffuse compared to the one observed for **4**. **D** is also much more persistent than its counterpart in the ester series and is clearly visible until X_2 reaches 0.7. **D** may indeed be an overall negatively charged Coulomb complex with a formal 1 : 1 composition of **5** and **2**. Starting with $X_2 = 0.6$, free porphyrin **2** appears on the cathodic side of the plate (**E**).

2.6 Aggregation of the octacationic zinc porphyrin 2 with anionic dendrofullerene [3:3]hexakis adduct 6. The self-aggregation phenomenon of the [3:3]-hexakis adduct **6** is more pronounced than that of the dendrofullerene monoadducts **3**, **4**, and **5** because of its more balanced ratio of polar and unpolar moieties.

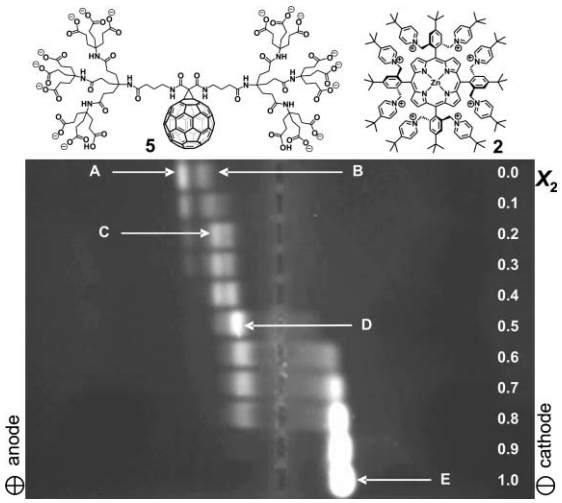

Fig. 7 Flat gel electrophoresis (PA-gel plate 100 mm × 65 mm × 5 mm; phosphate buffer, pH 7.2, 300 V, 12 mA, 273 K, 20 min) of a mixture of water-soluble dendrofullerene amide **5** and cationic zinc porphyrin **2** with increasing molar fraction of porphyrin X_2. Detection was performed with a long-pass filter. Gel pockets in the middle mark the starting points of electrophoresis. **A** and **B**: **5** is migrating towards the anodic region; **C** and **D**: anionic Coulomb aggregates migrate to the anode; **E**: **2** migrates to the cathode.

Consequently, compound **6** forms more stable micelle-like species. At this point, it was not clear how such a molecule would behave in complexation experiments with the cationic zinc porphyrin **2**.

Pure **6**, in contrast to **3**, **4** and **5**, shows just one band (**A**) on the electrophoresis plate, which is only detectable with the short- and medium-pass filters (Fig. 8a). With the long-pass filter (see Fig. 8b) **6** is not visible at all. The fact that **6** gives only one band is most likely due to a micelle-type aggregation. Because the fluorescence observed with the long-pass filter (Fig. 8b) originates solely from porphyrin **2**, the spots detected in the anodic compartment prove that **6** forms stable aggregates with **2**. In the anodic region, band **A** (which represents pure **6**) is detectable until the molar fraction of **2** reaches 0.3. Band **B** with a slower migration speed appears in the anodic region. It exists between $X_2 = 0.2$–0.8 with the most intense fluorescence in the range $X_2 = 0.5$–0.7. **B** must consist of aggregates of **6** and **2** in which an anionic 1 : 1 complex is the dominant species. In the cathodic region the porphyrin shows up (band **C**) at $X_2 = 0.7$. Interestingly, at this molar ratio, two distinct species can be observed. It is possible that the species evolving from **B** with increasing X_2 approaches a 1 : 2 complex of **6** and **2**, and thus can be found close to the center due to its more or less neutral status. Band **C** is due to free porphyrin **2**. Concluding this experiment, it is possible to identify two events in the electrophoresis that can be associated with the formation of 1 : 1 and 1 : 2 aggregates between **6** and **2**.

2.7 Aggregation of the octacationic zinc porphyrin 2 with anionic dendrofullerene [5:1]hexakis adduct 7. The dendritic part of the C_{60}–[5:1]-hexakis adduct **7** is identical to that of the dendrofullerene amide **5** and should be able to interact electrostatically with cationic chromophores such as **2**. The main body of the fullerene **7** is functionalized with alkylmalonates, giving the molecule an overall pronounced amphiphilic character. As already mentioned, the anionic fullerene **7** forms at pH 7.2 predominantly

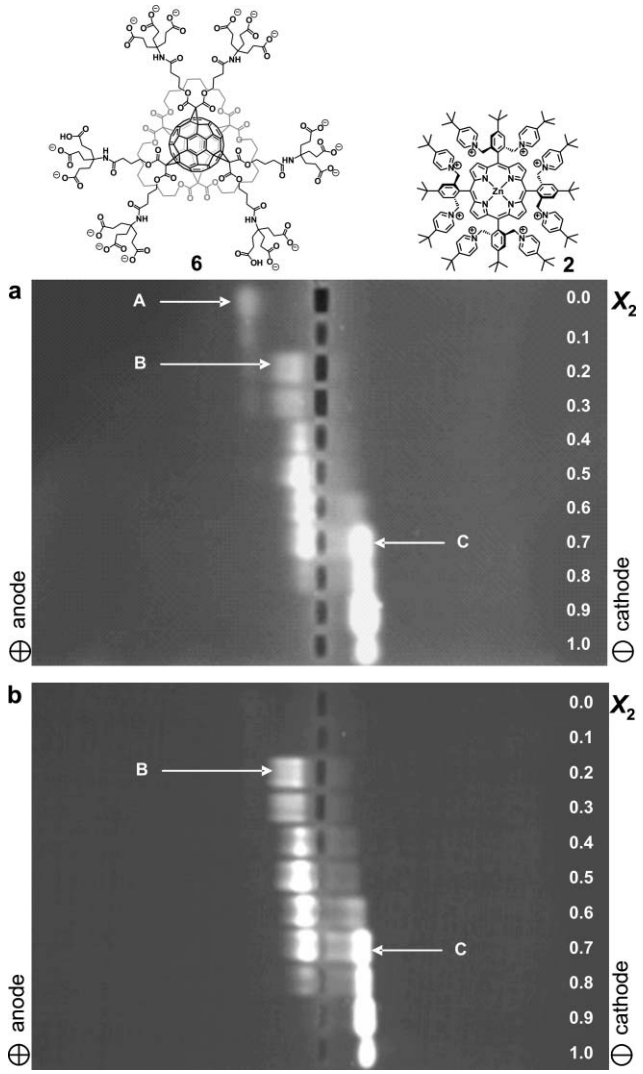

Fig. 8 Flat gel electrophoresis (PA-gel plate 100 mm × 65 mm × 5 mm; phosphate buffer, pH 7.2, 300 V, 12 mA, 273 K, 20 min) of a mixture of water-soluble dendrofullerene hexakis adduct **6** and cationic zinc porphyrin **2** with increasing molar fraction of porphyrin X_2; a) Detection was performed with a medium-pass filter. b) Detection was performed with a long-pass filter. Gel pockets in the middle mark the starting points of electrophoresis. **A**: **6** migrates to the anode; **B**: anionic Coulomb aggregates migrate to the anode; **C**: **2** migrates to the cathode.

rod-shaped aggregates with a double-layer ultrastructure. At pH 9.2 only globular micelles with a diameter of 85 ± 10 Å are formed. Although the concentrations used in the electrophoresis experiments are considerably lower than those used for the above-mentioned studies,[16] it is still reasonable to assume that **7** forms self-aggregates here, too.

Although **6** and **7** are comparable, at least on a first glance, **7** behaves remarkably differently in the electrophoresis experiment. Compound **7** shows three distinct bands (see Fig. 9) that are due to the presence of three discrete species. We believe the fastest migrating band (**A**) represents non-aggregated fullerene **7**, whereas the two other bands with slower movement (**B** and **C**) belong to aggregates of a size small enough to permeate through the polyacrylnitrile gel. This can only be true if the migration speed on the plate is dominated by the smaller size of a single fullerene entity

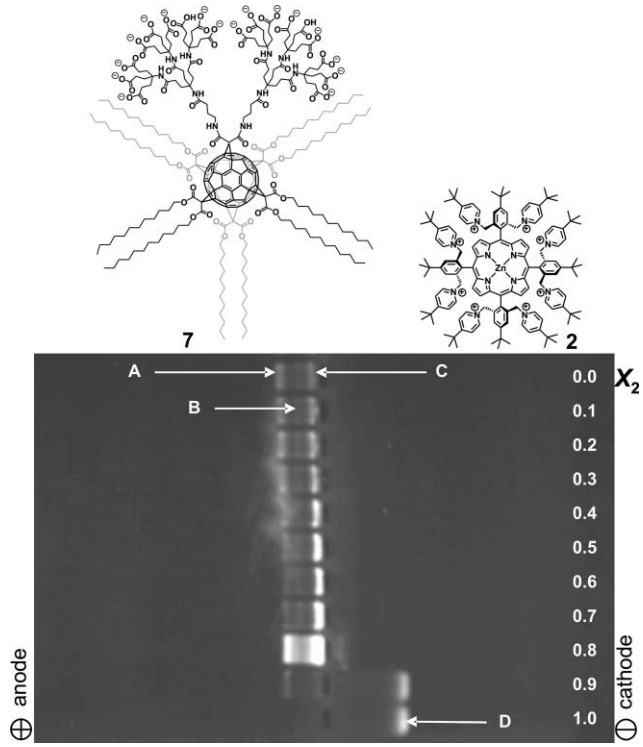

Fig. 9 Flat gel electrophoresis (PA-gel plate 100 mm × 65 mm × 5 mm; phosphate buffer, pH 7.2, 300 V, 12 mA, 273 K, 20 min) of a mixture of water-soluble dendrofullerene **7** and cationic zinc porphyrin **2** with increasing molar fraction of porphyrin X_2. Detection was performed with a long-pass filter. Gel pockets in the middle mark the starting points of electrophoresis. **A**, **B**, **C**: **7** is migrating towards the anodic region; **D**: **2** migrates to the anode. For $X_2 = 0.8$ the concentrations of **7** and **2** were doubled to be able to see even very small traces of **2**.

rather than by the higher total charge of the aggregated fullerenes. The picture becomes confusing when porphyrin **2** is added. Band **A** remains visible over the whole range of X_2, which indicates a lesser tendency of the fastest moving species to interact with cationic **2**. In contrast, band **B** vanishes with increasing amount of porphyrin **2**, which may be the result of a break-up of meta-stable aggregates under electrophoretic conditions. The third band **C** penetrates the gel only a few millimeters but the fluorescence intensity increases constantly until X_2 reaches 0.8, and than disappears completely. In the cathodic region, free porphyrin **2** can only be detected when $X_2 > 0.8$. At $X_2 = 0.8$ in Fig. 8, the concentrations of both compounds **2** and **7** were doubled to see if any porphyrin at all was detectable on the cathodic side, which obviously is not the case. The expected 1 : 2 or 1 : 1 complexes between **7** and **2** are not distinguished on the plate – in contrast to the previously discussed compounds. Nevertheless, since no precipitate is observed in the pockets but discrete migrating bands are seen, we believe that more or less well-defined aggregates exist. It seems reasonable to assume that **C** consists of large micellar structures of **7** that have attracted increasing amounts of **2**, giving complexes that migrate slowly due to their size.

Conclusions

We have shown that gel electrophoresis with conditions as decribed allowed for the observation of electrostatic complexation events between fullerene and porphyrin oligoelectrolytes. A variation of detection modes – short-, medium-, and long-pass filters – gave a better insight into the processes and made the separation of individual species and aggregation phenomena possible. Depending on the compounds, the formation of discrete 1 : 1 or 2 : 1 aggregates was seen, although the picture was not necessarily simple. In particular, our experiments have demonstrated that fullerene carboxylate **3** forms more stable complexes with cationic porphyrin **2** than with ferric cytochrome c **1**. Although this conclusion is drawn on a qualitative level, gel electrophoretic studies nevertheless reproduced the results obtained with UV/Vis and fluorescence spectroscopic techniques for a similar fullerene derivative with both cationic species **1** and **2**.[4,5]

With increasing amphiphilicity the formation of self-aggregates was found to be more and more pronounced in the electrophoresis experiments. These observations are in accord with, for example, DOSY measurements at higher concentrations. Interestingly, the behaviour of **7** in complexation studies indicated that the preformed aggregates are stable even when porphyrin **2** was added.

In conclusion, we have presented in this study the advantages and limitations of gel electrophoresis in analysing the electrostatic complexation of chromophoric oligoelectrolytes. Whereas the precise nature of these complexes may leave room for interpretation, the complexation events as such can be detected without any doubt.

Experimental

General

Ferric cytochrome c **1**, Na_2HPO_4 and NaH_2PO_4 were purchased from Fluka and were used as received. Acrylamide, methylenebisacrylamide, ammonium peroxidisulfate (APS), *N*,*N*,*N*′,*N*′,-tetramethylethylenediamine (TEMED), *N*‴-*tert*-butyl-*N*,*N*,*N*′,*N*′,*N*″,*N*″-hexamethylphosphorimide triamide acid (phosphazene P_1-base) were purchased from Sigma–Aldrich and were also used as received. C_{60} was obtained as a gift from Hoechst AG/Aventis and separated from higher fullerenes by plug filtration.[24] All analytical reagent-grade solvents were purified by distillation. Dry solvents were prepared using customary literature procedures.[25]

Compound **2**[26] and the charged dendrofullerenes **4**,[14] **5**,[15,16] and **7**[16] were prepared according to published literature methods. The buffers were prepared by dissolving the appropriate amount of Na_2HPO_4 and NaH_2PO_4 in doubly distilled water.

NMR spectra: JEOL JNM EX 400, JEOL JNM GX 400, Bruker AVANCE 300, Bruker AVANCE 400. The chemical shifts are given in ppm relative to $SiMe_4$ (TMS). The resonance multiplicities are indicated as s (singlet), d (doublet), t (triplet), q (quartet) and m (multiplet), broad resonances as br. The abbreviations dend, int and ex refer to atoms of the dendrimer, internal C atoms of the dendrimer and external C atoms of the dendrimers, respectively. The term quart is used for quarternary C-atoms. UV/Vis Spectra: Shimadzu UV-3102 PC, UV/Vis-NIR scanning spectrophotometer. IR spectra: Bruker FT-IR Vector 22, KBr pellets or thin film (NaCl plates). Mass spectra: Micromass Zabspec, FAB (LSIMS) mode (3-nitrobenzylalcohol); Gel electrophoresis: Hoefer HE 33 Mini Submarine Unit. Detection was performed with a GeneGenius gel documentation system from Syngene including a darkroom with a transilluminator with a

single wave length emission of 303 nm. The gels were photographed with a 16-bit CCD-camera with an appropriate lens filter system including short-pass (sp) 500–550 nm, medium-pass (mp) 550–610 nm and long-pass (lp) 600–650 nm filters. Analyses of the gels were performed with GeneTools Analysis software.

Sample preparation of the gel electrophoreses

Stock solutions of the samples (10^{-3} M) were prepared by dissolving 1.0 μmol in 1.0 mL phosphate buffer (pH 7.2, I = 0.012). The stock solutions were diluted according to the different spectroscopic properties of the compounds used to ensure proper detection. The molar fractions of different polycationic and polyanionic derivatives were prepared, and a small drop of glycerol was added to each fraction.

Preparations of the PA-gels were performed according to the following procedure: the pore size is exactly and reproducibly controlled by the total acrylamide concentration T and the degree of crosslinking C. A stock solution consisting of 28.5 g monomeric acrylamide and 1.5 g methylene bisacrylamide dissolved in 100 mL doubly distilled water (representing T = 30% and C = 5%) was prepared. Polymerization of the gel was carried out by mixing 2.5 parts of the stock solution, 1.0 part of phosphate buffer and 6.0 parts of water followed by the addition of 80 μL APS and 80 μL TEMED. The gels were ready to use after two hours.

Best results were obtained in a phosphate buffer (pH 7.2) with appropriate ionic strength so that the current was held at a low level. During electrophoresis the horizontal device was cooled to 0 °C. The gel pockets were loaded with 5–10 μL of the different molar fractions. Electrophoresis runs were performed on a 20–30 min time range.

Syntheses

Mono-1-(3-(*tert*-butoxycarbonyl)propyl) malonate 10. To a stirred solution of malonic acid (0.97 g, 9.32 mmol) and *tert*-butyl 4-hydroxybutyrate (1.50 g, 9.38 mmol) in absolute CH_2Cl_2 at −40 °C was added a solution of DCC (1.92 g, 9.32 mmol) in CH_2Cl_2. The mixture was stirred for 2 h at −40 °C and then overnight at room temperature. The insoluble materials were removed by filtration. The filtrate was evaporated to give a residue, which was taken up into a mixture of dilute aqueous $NaHCO_3$ and Et_2O. The aqueous layer was further washed with Et_2O and then acidified with conc. HCl. After extraction with Et_2O several times, the combined extract was dried and concentrated, affording 1.20 g (4.85 mmol; 52%) of the half-ester as a transparent oil; ^{1}H NMR (300 MHz, $CDCl_3$, rt): δ = 4.20 (t, ^3J = 6.4 Hz, 2H, OCH_2CH$_2$), 3.43 (s, 2H, OOCCH_2COO), 2.32 (t, ^3J = 7.4 Hz, 2H, CH_2COOC(CH$_3$)$_3$), 1.95 (m, 2H, CH$_2$CH_2CH$_2$), 1.45 (s, 9H, C(CH_3)$_3$); ^{13}C NMR (75.5 MHz, $CDCl_3$, rt): δ = 172.32 (*C*=O), 170.57 (*C*=O), 166.82 (*C*=O), 80.80 (*C*(CH$_3$)$_3$), 64.83 (O*C*H$_2$CH$_2$), 40.77 (OOC*C*H$_2$COO), 31.75 (*C*H$_2$COOC(CH$_3$)$_3$), 28.00 (C(*C*H$_3$)$_3$), 23.88 (CH$_2$*C*H$_2$CH$_2$); MS (FAB, NBA): *m*/*z*: 247 [M]$^+$, 269 [M + Na]$^+$; $C_{11}H_{18}O_6$, calcd: C 53.65, H 7.37; found: C 53.66, H 7.36.

Malonate derivative 11. To a stirred solution of the monoester **10** (0.73 g, 2.97 mmol) and triethylene glycol monomethyl ether (0.50 g, 3.04 mmol) in absolute CH_2Cl_2 at 0 °C was added a solution of DCC (0.65 g, 3.15 mmol) in CH_2Cl_2, and the mixture was stirred overnight at room temperature. After filtration, the filtrate was evaporated to give a residue, which was taken up into a mixture of dilute aqueous $NaHCO_3$ and Et_2O. The organic layer was washed successively with aqueous $NaHCO_3$ and brine, dried and concentrated, affording 0.50 g (1.27 mmol; 43%) of the desired malonate derivative as a transparent oil; ^{1}H NMR (400 MHz, $CDCl_3$, rt): δ = 4.21 (t, ^3J = 4.8 Hz, 2H, COOCH_2CH$_2$O), 4.08 (t, ^3J = 6.4 Hz, 2H, COOCH_2CH$_2$CH$_2$), 3.62 (t, ^3J = 4.8 Hz, 2H, COOCH$_2$CH_2O), 3.55 (m, 6H, OCH_2), 3.45 (m, 2H, OCH_2), 3.32 (s, 2H, OOCCH_2COO), 3.28 (s, 3H, OCH_3), 2.21 (t, ^3J = 7.4 Hz, 2H, CH_2COO), 1.84 (q, ^3J = 6.9 Hz, 2H, CH_2CH$_2$COO); ^{13}C NMR (100.5 MHz, $CDCl_3$, rt): δ = 171.80 (1C, *C*=O), 166.31 (1C, *C*=O), 166.18 (1C, *C*=O), 80.29 (1C, *C*(CH$_3$)$_3$), 71.70 (1C, *C*H$_2$OCH$_3$), 70.38 (2C, O*C*H$_2$), 70.35 (1C, O*C*H$_2$), 68.61 (1C, OOCCH$_2$*C*H$_2$), 64.37 (1C, COO*C*H$_2$), 64.36 (1C, COO*C*H$_2$), 58.80 (1C, O*C*H$_3$), 41.14 (1C, OOC*C*H$_2$COO), 31.54 (1C, *C*H$_2$COO), 27.87 (3C, C(*C*H$_3$)$_3$), 23.78 (1C, *C*H$_2$CH$_2$COO); MS (FAB, NBA): *m*/*z*: 393 (M$^+$).

Malonate derivative 12. A solution of malonate **11** (150 mg, 0.382 mmol) in formic acid was stirred for 20 h at room temperature, and the progress of the reaction monitored by TLC. The mixture was concentrated and dried *in vacuo* to afford 127 mg (0.378 mmol; 99%) of the product as a colorless oil. ^{1}H NMR (300 MHz, $CDCl_3$, rt): δ = 9.38 (br, 1H, COO*H*), 4.25 (t, ^3J = 4.7 Hz, 2H, COOCH_2CH$_2$O), 4.08 (t, ^3J = 6.1 Hz, 2H, COOCH_2CH$_2$CH$_2$), 3.67 (t, ^3J = 4.7 Hz, 2H, COOCH$_2$CH_2O), 3.59 (m, 6H, OCH_2), 3.51 (m, 2H, OCH_2), 3.36 (s, 2H, OOCCH_2COO), 3.33 (s, 3H, OCH_3), 2.39 (t, ^3J = 7.0 Hz, 2H, CH_2COOH), 1.94 (q, ^3J = 6.6 Hz, 2H, CH_2CH$_2$COOH); ^{13}C NMR (75.5 MHz, $CDCl_3$, rt): δ = 177.31 (1C, *C*=O), 166.40 (1C, *C*=O), 166.26 (1C, *C*=O), 71.73 (1C, *C*H$_2$OCH$_3$), 70.40 (1C, O*C*H$_2$), 70.37 (1C, O*C*H$_2$), 70.30 (1C, O*C*H$_2$), 68.72 (1C, OOCCH$_2$*C*H$_2$), 64.49 (1C, COO*C*H$_2$), 64.29 (1C, COO*C*H$_2$), 58.83 (1C, O*C*H$_3$), 41.25 (1C, OOC*C*H$_2$COO), 30.22 (1C, *C*H$_2$COO), 23.52 (1C, *C*H$_2$CH$_2$COO); MS (FAB, NBA): *m*/*z*: 337 (M$^+$), 359 (M + Na$^+$).

Malonate derivative 13. A solution of 1-ethyl-3-(3-dimethylaminopropyl)carbodiimide (43 mg, 0.222 mmol) was added to a cooled solution (0 °C) of malonate **12** (50 mg, 0.148 mmol), dendron H_2N–G2 (0.256 g, 0.178 mmol), DMAP (18.1 mg, 0.148 mmol) and 1-hydroxybenzotriazole (24.1 mg, 0.178 mmol) in dry THF (40 mL) under a nitrogen atmosphere. The reaction mixture was stirred for 20 h at room temperature, and the progress of the reaction monitored by TLC. The reaction mixture was diluted with 100 mL of CH_2Cl_2 and extracted twice with water. After drying and concentration of the organic residue, the product was isolated by flash chromatography (silica gel, CH_2Cl_2–ethyl acetate 3 : 2 to 1 : 2) and dried *in vacuo*, affording 128 mg (0.111 mmol; 50%) of a white solid. ^{1}H NMR (300 MHz, $CDCl_3$, rt): δ = 7.17 (br, 1H, N*H*), 6.06 (br, 3H, N*H*), 4.26 (t, ^3J = 4.5 Hz, 2H, COOCH_2CH$_2$O), 4.16 (t, ^3J = 5.9 Hz, 2H, COOCH_2CH$_2$CH$_2$), 3.67 (t, ^3J = 4.5 Hz, 2H, COOCH$_2$CH_2O), 3.59 (m, 6H, OCH_2), 3.50 (m, 2H, OCH_2), 3.41 (s, 2H, OOCCH_2COO), 3.32 (s, 3H, OCH_3), 2.62 (m, 2H, CH_2CONH), 2.10 (m, 26H, CH_2CH$_2$CONH, CH_2-dend-CONH, CH_2-dend-COO), 1.87 (m, 24H, CH_2CH$_2$-dend-CONH, CH_2CH$_2$-dend-COO), 1.37 (s, 81H, C(CH_3)$_3$); ^{13}C NMR (75.5 MHz, $CDCl_3$, rt): δ = 172.62 (3C, *C*ONH), 172.57 (9C, *C*=O), 171.65 (1C, *C*ONH),

166.86 (1C, *C*=O), 166.82 (1C, *C*=O), 80.41 (9C, *C*(CH_3)$_3$), 71.81 (1C, *C*H_2OCH$_3$), 70.44 (3C, O*C*H_2), 68.75 (1C, OOCCH_2*C*H_2), 64.67 (1C, COO*C*H_2), 64.30 (1C, COO*C*H_2), 58.92 (1C, O*C*H_3), 57.58 (1C, NH*C*$_{quart\text{-}int}$), 57.26 (3C, NH*C*$_{quart\text{-}ex}$), 41.33 (1C, OO*C*H_2COO), 32.41 (1C, *C*H_2CONH), 31.47, 31.43 (6C, int-*C*H_2-dend), 29.70, 29.65 (18C, ex-*C*H_2-dend), 27.99 (27C, C(*C*H_3)$_3$), 24.22 (1C, *C*H_2CH$_2$CONH); MS (FAB, NBA): *m*/*z*: 1759 (M^+).

Monoadduct 14. DBU (13.5 mg, 13.3 μL, 0.0887 mmol) was added dropwise to a solution of C_{60} (63.9 mg, 0.089 mmol), malonate derivative **13** (120 mg, 0.0683 mmol) and iodine (19.1 mg, 0.075 mmol) in dry toluene (1 L) under a nitrogen atmosphere. The reaction mixture was stirred at room temperature for 20 h and the progress of the reaction was monitored by TLC. The product was isolated by flash chromatography (silica gel, toluene) and dried *in vacuo*, affording 72.7 mg (0.0294 mmol; 42%) of a brownish-red solid. ^{1}H NMR (400 MHz, $CDCl_3$, rt): δ = 7.35 (br, 1H, N*H*), 6.09 (br, 3H, N*H*), 4.63 (t, ^3J = 4.5 Hz, 2H, COOC*H*$_2$CH$_2$O), 4.50 (t, ^3J = 6.2 Hz, 2H, COOC*H*$_2$CH$_2$CH$_2$), 3.84 (t, ^3J = 4.5 Hz, 2H, COOCH$_2$C*H*$_2$O), 3.65 (m, 6H, OC*H*$_2$), 3.49 (m, 2H, OC*H*$_2$), 3.31 (s, 3H, OC*H*$_3$), 2.31 (m, 2H, C*H*$_2$CONH), 2.13 (m, 26H, C*H*$_2$CH$_2$CONH, C*H*$_2$-dend-CONH, C*H*$_2$-dend-COO), 1.90 (m, 24H, C*H*$_2$CH$_2$-dend-CONH, C*H*$_2$CH$_2$-dend-COO), 1.37 (s, 81H, C(C*H*$_3$)$_3$); ^{13}C NMR (100.5 MHz, $CDCl_3$, rt): δ = 172.63 (3C, *C*ONH), 172.51 (9C, *C*=O), 171.48 (1C, *C*ONH), 163.66 (1C, *C*=O), 163.49 (1C, *C*=O), 145.15, 145.14, 145.12, 145.07, 145.05, 145.03, 145.01, 144.76, 144.57, 144.53, 144.52, 144.49, 144.48, 143.75, 142.93, 142.92, 142.88, 142.85, 142.09, 142.05, 141.79, 141.71, 140.86, 140.75, 139.05, 138.89 (58C, sp^2-*C*), 80.41 (9C, *C*(CH$_3$)$_3$), 71.81 (1C, *C*H$_2$OCH$_3$), 71.35 (1C, sp^3-*C*), 70.48 (1C, sp^3-*C*), 70.44 (3C, O*C*H$_2$), 68.67 (1C, OOCCH$_2$*C*H$_2$), 66.62 (1C, COO*C*H$_2$), 66.24 (1C, COO*C*H$_2$), 58.89 (1C, O*C*H$_3$), 57.54 (1C, NH*C*$_{quart\text{-}int}$), 57.32 (3C, NH*C*$_{quart\text{-}ex}$), 52.07 (1C, OOC*C*COO), 32.45 (1C, *C*H$_2$CONH), 31.53, 31.44 (6C, int-*C*H$_2$-dend), 29.71, 29.66 (18C, ex-*C*H$_2$-dend), 27.99 (27C, C(*C*H$_3$)$_3$), 24.24 (1C, *C*H$_2$CH$_2$CONH); UV/Vis (CH_2Cl_2): λ_{max}/nm (ε/cm^{-1} M^{-1}) = 256 (92 000), 323 (33 000), 425 (2700) 470 (1900); MS (FAB, NBA): *m*/*z*: 2477 (M^+), 2500 (M + Na^+), 2609 (M + Cs^+).

Monoadduct 15. A solution of monoadduct **14** (70 mg, 0.028 mmol) in formic acid was stirred for 20 h at room temperature, and the progress of the reaction monitored by TLC. The mixture was concentrated and dried *in vacuo* to afford 55 mg (0.028 mmol; 99%) of the product as a brownish-red solid. ^{1}H NMR (400 MHz, DMSO-d_6, rt): δ = 7.27 (br, 3H, N*H*), 7.20 (br, 1H, N*H*), 4.64 (m, 2H, COOC*H*$_2$CH$_2$O), 4.51 (m, 2H, COOC*H*$_2$CH$_2$CH$_2$), 3.80 (m, 2H, COOCH$_2$C*H*$_2$O), 3.53 (m, 6H, OC*H*$_2$), 3.42 (m, 2H, OC*H*$_2$), 3.21 (s, 3H, OC*H*$_3$), 2.24 (m, 2H, C*H*$_2$CONH), 2.10 (m, 26H, C*H*$_2$CH$_2$CONH, C*H*$_2$-dend-CONH, C*H*$_2$-dend-COOH), 1.84 (m, 24H, (C*H*$_2$CH$_2$-dend-CONH, C*H*$_2$CH$_2$-dend-COOH); ^{13}C NMR (100.5 MHz, DMSO-d_6, rt): δ = 174.48 (9C, *C*OOH), 172.21 (3C, *C*ONH), 170.72 (1C, *C*ONH), 162.75 (1C, *C*=O), 162.66 (1C, *C*=O), 145.15, 144.80, 144.74, 144.65, 144.62, 144.31, 144.21, 144.14, 144.10, 144.04, 143.39, 142.50, 142.47, 141.79, 141.71, 141.38, 141.32, 140.56, 140.36, 138.54, 138.41 (58C, sp^2-*C*), 71.36 (1C, *C*H$_2$OCH$_3$), 71.23 (1C, sp^3-*C*), 69.84 (1C, sp^3-*C*), 69.73 (3C, O*C*H$_2$), 69.58 (1C, OOCCH$_2$*C*H$_2$), 68.08 (1C, COO*C*H$_2$), 66.52 (1C, COO*C*H$_2$), 58.09 (1C, O*C*H$_3$), 56.78 (1C, NH*C*$_{quart\text{-}int}$), 56.32 (3C, NH*C*$_{quart\text{-}ext}$), 52.33 (1C, OOC*C*COO), 33.31 (1C, *C*H$_2$CONH), 30.75, 30.29 (6C, int-*C*H$_2$-dend), 29.12, 28.09 (18C, ex-*C*H$_2$-dend), 24.45 (1C, *C*H$_2$CH$_2$CONH); UV/Vis (H_2O, pH 7.2 phosphate buffer): λ_{max}/nm (ε/cm^{-1} M^{-1}) = 253 (84 000), 321 (33 000), 424 (3700); MS (FAB, NBA): *m*/*z*: 720 (C_{60}), 1972 (M^+), 1995 (M + Na^+).

[G1]-malonate 17. The reaction was carried out under a nitrogen atmosphere. A solution of dicyclohexylcarbodiimide (785 mg, 3.805 mmol) and 1-hydroxybenzotriazole (583 mg, 3.805 mmol) in dry THF were added successively to a cooled solution (0 °C) of diacid **16** (300 mg, 1.087 mmol) and dendron H_2N–G1 (1000 mg, 2.391 mmol) in dry THF (25 mL) under a nitrogen atmosphere. The reaction mixture was stirred for 2 h at 0 °C followed by stirring for 15 h at room temperature, and the progress of the reaction monitored by TLC. The insoluble materials were removed by filtration. The filtrate was concentrated *in vacuo*, diluted with a small amount of cooled EtOAc, and was once more filtered to give a residue, which was successively washed with 10% HCl, water, a saturated solution of $NaHCO_3$ and finally with brine. After drying over $MgSO_4$, filtering and concentrating, purification was carried out by flash chromatography (silica gel, hexane–ethyl acetate 2 : 3 to 1 : 1). The purified material was dried *in vacuo*, affording 758 mg (0.708 mmol; 65%) of a transparent highly viscous oil. ^{1}H NMR (400 MHz, $CDCl_3$, rt): δ = 6.05 (br, 2H, N*H*), 4.15 (t, ^3J = 6.2 Hz, 4H, OC*H*$_2$), 3.36 (s, 2H, OOCC*H*$_2$COO), 2.17 (m, 16H, C*H*$_2$CONH, C*H*$_2$COO), 1.93 (m, 16H, C*H*$_2$CH$_2$CONH, C*H*$_2$CH$_2$COO), 1.39 (s, 54H, C(C*H*$_3$)$_3$); ^{13}C NMR (100.5 MHz, $CDCl_3$, rt): δ = 173.30 (6C, *C*=O), 171.69 (2C, *C*=O), 167.11 (2C, *C*ONH), 80.61 (2C, *C*(CH$_3$)$_3$), 64.59 (2C, O*C*H$_2$), 57.31 (2C, NH*C*$_{quart}$), 41.20 (1C, OOC*C*H$_2$COO), 32.98 (2C, *C*H$_2$CONH), 29.61 (12C, int-*C*H$_2$-dend), 29.50 (12C, ex-*C*H$_2$-dend), 27.77 (18C, C(*C*H$_3$)$_3$), 24.26 (2C, *C*H$_2$CH$_2$CONH); MS (FAB, NBA): *m*/*z*: 1071 (M^+), 1094 (M + Na^+).

[3:3]-(*eee*-[G1])-hexakis adduct 19. The reaction was carried out under nitrogen atmosphere. The *eee*-trisadduct **18** (106 mg, 77.8 μmol) was dissolved in dry CH_2Cl_2 (40 mL). DMA (96 mg, 467 μmol) was added to the solution and stirred for 2 h at ambient temperature. CBr_4 (155 mg, 467 μmol) and malonate-G1 **17** (500 mg, 467 μmol) were added subsequently. After stirring a few minutes to allow complete dissolution, P_1-base (218 μL, 857 μmol) was diluted with dry CH_2Cl_2 (25 mL) and added dropwise over a period of 1 h. The solution was stirred for 2 days at room temperature in the dark until the TLC remained unchanged. The reaction was quenched with diluted HCl. After extracting with water followed by drying over $MgSO_4$, filtering and concentrating, purification was carried out by flash chromatography (silica gel, hexane–ethyl acetate 2 : 1 to 1 : 1). The product fractions were evaporated, precipitated from CH_2Cl_2–pentane, centrifuged, washed with pentane and dried *in vacuo*. 152 mg of a yellow crystalline material was obtained (33.3 μmol; 43%). ^{1}H NMR (400 MHz, $CDCl_3$, rt): δ = 6.34 (br, 3H, N*H*), 6.29 (br, 3H, N*H*), 4.69, 4.34, 4.22, 4.15, 4.01 (5m, 24H, OC*H*$_2$), 2.21 (m, 48H, C*H*$_2$CONH, int-C*H*$_2$-dend), 1.97 (m, 48H, C*H*$_2$CH$_2$CONH, ex-C*H*$_2$-dend), 1.81, 1.55 (2m, 15H, C*H*$_2$-macrocycle), 1.42 (s, 162H, C(C*H*$_3$)$_3$), 1.15 (m, 18H, C*H*$_2$-macrocycle), 0.82 (m, 3H, C*H*$_2$-macrocycle). ^{13}C NMR (100.5 MHz, $CDCl_3$, rt): δ = 172.87 (18C, *C*=O), 171.36 (3C, *C*ONH), 171.16 (3C, *C*ONH), 163.83 (3C, *C*=O), 163.71 (3C, *C*=O), 163.52 (3C, *C*=O), 163.18 (3C, *C*=O), 146.51, 145.90, 145.83, 145.77, 145.27, 145.12, 144.93, 142.07, 141.97, 141.69, 140.97, 140.95, 140.82, 140.62 (48C, sp^2-*C*), 80.43 (9C,

$C(CH_3)_3$), 80.40 (9C, $C(CH_3)_3$), 69.22 (6C, sp^3-*C*), 69.14 (6C, sp^3-*C*), 67.05 (3C, O*C*H_2), 66.50 (3C, O*C*H_2), 66.23 (6C, O*C*H_2), 57.55 (3C, NH*C*$_{quart}$), 57.51 (3C, NH*C*$_{quart}$), 46.77 (3C, OOC*C*COO), 45.35 (3C, OOC*C*COO), 32.95 (3C, *C*H_2CONH), 32.82 (3C, *C*H_2CONH), 29.65 (36C, int-*C*H_2-dend), 29.62 (36C, ex-*C*H_2-dend), 29.25 (3C, *C*H_2), 29.11 (3C, *C*H_2), 28.78 (3C, *C*H_2), 28.00 (54C, C(*C*H_3)$_3$), 27.67 (3C, *C*H_2), 26.27 (3C, *C*H_2), 25.54 (3C, *C*H_2), 24.35 (3C, *C*H_2CH$_2$CONH), 24.01 (3C, *C*H_2CH$_2$CONH); UV/Vis (CH_2Cl_2): λ_{max}/nm (ε/cm^{-1} M^{-1}) = 270 (51 000), 281 (55 000), 316 (37 000) 334 (31 000); MS (FAB, NBA): *m*/*z*: 4565 (M^+), 4585 ($M + Na^+$).

Deprotected [3:3]-(*eee*-[G1])-hexakis adduct 20. Trifluoroacetic acid (6.0 mL, 78.0 mmol) was added to a solution of **19** (152 mg, 33.3 μmol) in dry CH_2Cl_2 (20 mL) under a nitrogen atmosphere. The reaction mixture was stirred for 15 h at room temperature, and the progress of the reaction monitored by TLC. The reaction mixture was concentrated and dried *in vacuo* to afford 118 mg (33.2 μmol; 99%) of the product as a yellow crystalline solid. ^{1}H NMR (400 MHz, CD_3OD, rt): δ = 4.71, 4.38, 4.10, 4.02 (4m, 24H, OC*H*$_2$), 2.24 (m, 48H, C*H*$_2$CONH, int-C*H*$_2$-dend), 2.01 (m, 48H, C*H*$_2$CH$_2$CONH, ex-C*H*$_2$-dend), 1.82, 1.53, 1.40, (3m, 15H, C*H*$_2$-macrocycle), 1.21 (m, 18H, C*H*$_2$-macrocycle), 0.81 (m, 3H, C*H*$_2$-macrocycle); ^{13}C NMR (100.5 MHz, CD_3OD, rt): δ = 177.39 (9C, *C*OOH), 177.31 (9C, *C*OOH), 174.68 (3C, *C*ONH), 174.55 (3C, *C*ONH), 165.19 (3C, *C*=O), 165.01 (3C, *C*=O), 164.49 (3C, *C*=O), 164.18 (3C, *C*=O), 147.55, 147.21, 147.11, 146.74, 146.58, 146.30, 146.01, 143.63, 143.58, 143.13, 143.05, 142.64, 142.46, 142.41 (48C, sp^2-*C*), 70.93 (3C, sp^3-*C*), 70.87 (3C, sp^3-*C*), 70.78 (3C, sp^3-*C*), 70.71 (3C, sp^3-*C*), 68.56 (3C, O*C*H_2), 67.83 (6C, O*C*H_2), 67.26 (3C, O*C*H_2), 58.80 (6C, NH*C*$_{quart}$), 47.59 (6C, OOC*C*COO), 33.90 (3C, *C*H_2CONH), 33.81 (3C, *C*H_2CONH), 30.91 (3C, *C*H_2), 30.47 (36C, int-*C*H_2-dend), 30.14 (6C, *C*H_2), 30.05 (3C, *C*H_2), 29.28 (36C, ex-*C*H_2-dend), 27.71 (3C, *C*H_2), 26.89 (3C, *C*H_2), 25.94 (6C, *C*H_2CH$_2$CONH; UV/Vis (H_2O, pH 7.2 phosphate buffer): λ_{max}/nm (ε/cm^{-1} M^{-1}) = 270 (55 000), 280 (58 000), 317 (37 000) 333 (31 000); MS (FAB, NBA): *m*/*z*: 3557 (M^+), 3580 ($M + Na^+$).

Acknowledgements

We gratefully acknowledge financial support by the Deutsche Forschungsgemeinschaft (SFB 583, Redoxactive Metal Complexes).

References

1 S. S. Isied, G. Worosila and S. J. Arterton, *J. Am. Chem. Soc.*, 1982, **104**, 7659–7661; S. S. Isied, *Adv. Chem. Ser.*, 1997, **253**, 331–347; J. V. McArdle, H. B. Gray, C. Creutz and N. Sutin, *J. Am. Chem. Soc.*, 1974, **96**, 5737–5741; J. V. McArdle, K. Yocom and H. B. Gray, *J. Am. Chem. Soc.*, 1977, **12**, 4141–4145; M. Meier and R. van Eldik, *Inorg. Chim. Acta*, 1994, **225**, 95–101; M. Meier, R. van Eldik, I. J. Chang, G. A. Mines, S. D. Wuttke, J. R. Winkler and H. B. Gray, *J. Am. Chem. Soc.*, 1994, **116**, 1577–1578; M. Meier, J. Sun, R. van Eldik and J. F. Wishart, *Inorg. Chim. Acta*, 1996, **35**, 1564–1570; M. Meier and R. van Eldik, *Inorg. Chim. Acta*, 1996, **242**, 185–189; M. Meier and R. van Eldik, *Chem. Eur. J.*, 1997, **3**, 39–46.
2 R. K. Jain and A. D. Hamilton, *Angew. Chem., Int. Ed.*, 2002, **41**, 641–643.
3 G. Decher, *Science*, 1997, **277**, 1232–1237; D. M. Kaschak, J.-T. Lehn, C. C. Waraksa, G. B. Saupe, H. Usami and T. E. Mallouk, *J. Am. Chem. Soc.*, 1999, **121**, 3435–3445.
4 M. Braun, S. Atalick, D. M. Guldi, H. Lanig, M. Brettreich, S. Burghardt, M. Hatzimarinaki, E. Ravanelli, M. Prato, R. van Eldik and A. Hirsch, *Chem. Eur. J.*, 2003, **9**, 3867–3875.
5 D. Balbinot, S. Atalick, D. M. Guldi, M. Hatzimarinaki, A. Hirsch and N. Jux, *J. Phys. Chem. B*, 2003, **107**, 13273–13279.
6 D. M. Guldi, A. M. G. Rahman, N. Jux, D. Balbinot, U. Hartnagel, N. Tagmatarchis and M. Prato, *J. Am. Chem. Soc.*, 2005, **127**, 9830–9838; D. M. Guldi, A. M. G. Rahman, M. Prato, N. Jux, Q. Shuhui and F. Warren, *Angew. Chem., Int. Ed.*, 2005, **44**, 2015–2018; D. M. Guldi, A. M. G. Rahman, N. Jux, D. Balbinot, N. Tagmatarchis and M. Prato, *Chem. Commun.*, 2005, **15**, 2038–2040; D. M. Guldi, A. M. G. Rahman, N. Jux, N. Tagmatarchis and M. Prato, *Angew. Chem., Int. Ed.*, 2004, **43**, 5526–5530; D. M. Guldi, A. M. G. Rahman, J. Ramey, M. Marcaccio, D. Paolucci, F. Paolucci, Q. Shuhui, F. Warren, D. Balbinot, N. Jux, N. Tagmatarchis and M. Prato, *Chem. Commun.*, 2004, **18**, 2034–2035; D. M. Guldi, I. Zilbermann, G. Anderson, A. Li, D. Balbinot, N. Jux, M. Hatzimarinaki, A. Hirsch and M. Prato, *Chem. Commun.*, 2004, **6**, 726–727.
7 J. W. Buchler and M. Nawra, *Inorg. Chem.*, 1994, **33**, 2830–2837.
8 J. W. Buchler and J. R. Simon, *Eur. J. Inorg. Chem.*, 2000, 2615–2621.
9 J.W. Buchler and M. Nawra, *Inorg. Chim. Acta*, 1996, **251**, 227–237.
10 S.-L. Tamisier-Karolak, S. Pagliarusco, C. Herrenknecht, M. Brettreich, A. Hirsch, R. Ceolin, R. V. Bensasson, H. Szwarc and F. Moussa, *Electrophoresis*, 2001, **22**, 4341–4346.
11 E. Nyarko and M. Tabata, *J. Porphyrins Phthalocyanines*, 2001, **5**, 873–880.
12 Ö. Almarsson, H. Adalsteinsson and T. C. Bruice, *J. Am. Chem. Soc.*, 1995, **117**, 4524–4532.
13 A. L. Mayburd, Y. Tan and J. Kassner, *Arch. Biochem. Biophys.*, 2000, **378**, 40–44.
14 M. Brettreich and A. Hirsch, *Tetrahedron Lett.*, 1998, **39**, 2731–2734.
15 S. Burghardt, *Ph.D. Dissertation*, University of Erlangen-Nuremberg, 2004.
16 S. Burghardt, A. Hirsch, B. Schade, K. Ludwig and C. Böttcher, *Angew. Chem., Int. Ed.*, 2005, **44**, 2976–2979.
17 G. Höfle and W. Steglich, *Synthesis*, 1972, 619–627; B. Neises and W. Steglich, *Angew. Chem., Int. Ed.*, 1978, **17**, 522–524; J. C. Sheehan and G. P. Hess, *J. Am. Chem. Soc.*, 1955, **77**, 1067; see also: Y. S. Klausen and M. Bodansky, *Synthesis*, 1972, 453 and citations therein.
18 G. R. Newkome, R. K. Behera, C. N. Moorefield and G. R. Baker, *J. Org. Chem.*, 1991, **56**, 7162–7167; G. R. Newkome, A. Nayak, R. K. Behera, C. N. Moorefield and G. R. Baker, *J. Org. Chem.*, 1991, **57**, 358–362.
19 U. Reuther, T. Brandmüller, W. Donaubauer, F. Hampel and A. Hirsch, *Chem. Eur. J.*, 2002, **8**, 2261–2273.
20 I. Lamparth, C. Maichle-Moessmer and A. Hirsch, *Angew. Chem., Int. Ed. Engl.*, 1995, **34**, 1607–1609.
21 R. Schwesinger, C. Hasenfratz, H. Schlemper, L. Walz, E. M. Peters, K. Peters and H. G. von Schnering, *Angew. Chem., Int. Ed. Engl.*, 1993, **32**, 1361–1363; R. Schwesinger and H. Schlemper, *Angew. Chem., Int. Ed. Engl.*, 1987, **26**, 1167–1169.
22 M. Braun, U. Hartnagel, E. Ravanelli, B. Schade, C. Böttcher, O. Vostrowsky and A. Hirsch, *Eur. J. Org. Chem.*, 2004, 1983–2001.
23 M. Brettreich, *Ph.D. Dissertation*, University of Erlangen-Nuremberg, 2000.
24 U. Reuther, *Ph.D. Dissertation*, University of Erlangen-Nuremberg, 2001; L. Isaacs, A. Wehrsig and F. Diederich, *Helv. Chim. Acta*, 1993, **76**, 1231.
25 D. D. Perrin and W. L. F. Amarego, *Purification of Laboratory Chemicals* (3rd edn), Pergamon Press, Oxford, 1988.
26 N. Jux, *Org. Lett.*, 2000, **2**, 2129–2132.